Cubic Interpolated Pseudo Particle (CIP) – Thermal BGK Lattice Boltzmann Numerical Scheme for Solving Incompressible Thermal Fluid Flow Problem

Nor Azwadi Che Sidik and Mohd Rosdzimin Abdul Rahman
Faculty of Mechanical Engineering,
Universiti Teknologi Malaysia,
81300 Skudai, Johor, Malaysia
E-mail: azwadi@fkm.utm.my

ABSTRACT

In this paper, cubic interpolated pseudo particle–lattice Boltzmann model is applied to simulate the natural convection of air in enclosure at various Rayleigh numbers. The basic idea is to discretise the advection term in lattice Boltzmann governing equation and solved using finite difference cubic-interpolated-pseudo-particle method. In our approach, two-dimensional nine-velocity model is coupled with two-dimensional four-velocity model to represent density and internal energy density distribution function respectively. Good agreement was obtained between the present approach and those by previous studies using Navier-Stokes solver and conventional LBM. The proposed approach is also found to be an efficient and stable numerical scheme for solving natural convection heat transfer problem.

Keywords: Natural convection, cubic-interpolated-pseudo-particle, lattice Boltzmann method, natural convection

INTRODUCTION

Lattice Boltzmann model (LBM) was introduced as an alternative to traditional methods for numerically solving the Navier Stokes equations (Bernsdorf *et al*., 2000 and Azwadi *et al*., 2006). The standard LBM imposed for the sake of numerical stability, Langragian approach for the evolution of particle distribution function and restricts the direction of moving particles at a site. The LBM also ignores particle correlation and often use a simpler Bhatnagar-Gross-Krook (BGK) collision operator (Bhatnagar *et al*., 1954). However, even under these simplifications, LBM has demonstrated its ability to simulate flows in porous media (Bernsdorf *et al*., 2000), immiscible fluids (Martys *et al*., 1996), magneto-hydrodynamics (Chen *et al*., 1991), etc.

Historically, LBM was derived from the lattice gas automata (LGA) method (Frish *et al*., 1986). Consequently, the LBM inherits some featuresfrom its precursor, the LGA method. The dynamics of distribution function evolving on a lattice space consists of two main steps; collision, particle at the same site collide according to a set of hard sphere particle collisions rules; and streaming, particle move to the nearest node in the direction of its velocities. However, instead of using Boolean representation of particle in LGA, LBM uses real numbers represent the local ensemble-averaged particle distribution function, and only kinetic equations for the distribution function are solved. The number of discrete velocities determines the lattice structure of LBM models. In other words, the discretization of physical space is coupled with the discretization of momentum space. As a result, computational in LBM is only restricted with uniform lattice structure and second order accuracy in space and time (Azwadi *et al*., 2008).

Due to the restraint mentioned above, the standard LBM has great difficulty in simulating fluid flow problem under critical conditions such as high Reynolds number or high Rayleigh numbers. Since He *et al*. (He *et al*., 1997) and Abe (Abe, 1998) demonstrated that the lattice Boltzmann equation is a discretized form of the continuous Boltzmann equation and the discretization of physical space is not necessary coupled with the discretization of momentum space, any standard numerical techniques can serve the purpose of solving the discrete Boltzmann equation. The first finite different LBM (FDLBM) was due to Reider and Sterling (Reider *et al*., 1995), and was examined by Cao *et al*. (Cao *et al*., 1997) in more detail. The study of FDLBM is still in progress (Azwadi *et al*., 2008, Tolke *et al*., 1998). In the present paper, we proposed a coupling of the modified finite different method with the LBM. Cubic interpolated pseudo particle method is chosen to discretize the advection term in the LBM governing equation. The CIP method tries to construct a solution inside the grid cell close enough to the real solution of the given equation with some constraints (Takashi *et al*., 2001). This method has been widely applied to simulate shock wave, milk crown formation and laser induced evaporation problems (Takashi *et al*., 2001). Consequently, this approach can be applied for the simulation at various conditions with low spatial resolution together with acceptable accuracy. For the verification purpose, we simulated the natural convection heat transfer in a square cavity ranging Ra = 10^3 to Ra = 10^5 and compared the obtained results with those from the previous studies.

The rest of the paper is organized as follow. In section 2, we discuss the theory of thermal LBM. The double distribution function (DDF) model

proposed by He *et al.* (He *et al.*, 1998) is brought as a governing equation due to its excellent numerical stability and widely used in simulating thermal fluid flow problems. The details theory of CIP is discussed in section 3. Then the CIP method is first used to solve the one dimensional advection equation by approximating spatial quantities in the grid interval using cubic polynomial. In section 4, the advection term and non advection term in LBM governing equation is split in order to formulize the CIP-LBM thermal scheme. In section 5, we apply the proposed CIP-LBM scheme and simulate the phenomena of natural convection in a square cavity. The final section concludes this study.

THERMAL LATTICE BOLTZMANN METHOD

The governing equations for double distribution function thermal LBM, (DDFTLBM) are

$$\frac{\partial f}{\partial t} + \mathbf{c}\frac{\partial f}{\partial x} = \Omega(f) + F \tag{1}$$

$$\frac{\partial g}{\partial t} + \mathbf{c}\frac{\partial g}{\partial x} = \Omega(g) \tag{2}$$

where the density distribution function $f = f(x,t)$ is use to simulate the density and velocity fields and the internal energy density distribution function $g = g(x,c,t)$ is used to simulate the macroscopic temperature field. C, Ω and F are the microscopic velocity, collision term and external force respectively.

The collision term is very complicated and must be simplified in practical calculations. One such simplification is to replace the collision term by a single relaxation time BGK model (Bhatnagar *et al.*,1954) as follow:

$$\frac{\partial f}{\partial t} + \mathbf{c}\frac{\partial f}{\partial x} = \frac{1}{\tau_f}\left(f^{eq} - f\right) + F \tag{3}$$

$$\frac{\partial g}{\partial t} + \mathbf{c}\frac{\partial g}{\partial x} = \frac{1}{\tau_g}\left(g^{eq} - g\right) \quad . \tag{4}$$

Eqs. (3) and (4) are known as the evolution equation of the density and internal energy density distribution function respectively.

The discretised equilibrium distributions are defined as:

$$f_i^{eq} = \rho \omega_i \left[1 - 3(\mathbf{c}_i \cdot \mathbf{u}) + \frac{9}{2}(\mathbf{c}_i \cdot \mathbf{u})^2 - \frac{3}{2}\mathbf{u}^2 \right] \qquad (5)$$

$$g_i^{eq} = T \omega_i \left[1 - 3(\mathbf{c}_i \cdot \mathbf{u}) \right] \qquad (6)$$

The value of ω in Eqs (5) and (6) is depends on the direction of the microscopic velocity of the particle distribution function. For two-dimension nine-velocity model, (D2Q9) the value of w are, $w_1=4/9$, $w_{2-5}=1/9$, $w_{6-9}=1/36$ and for D2Q4, $w_{1-4}=1/4$.
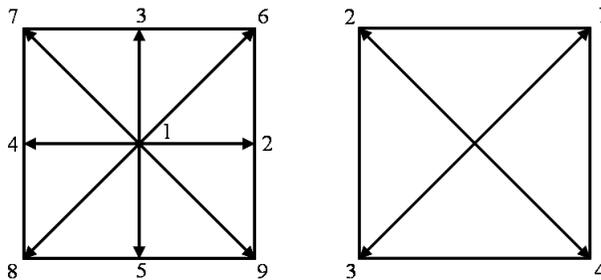

Figure 1: D2Q9 model (left) and D2Q4 model (right)

The macroscopic variables can be evaluated as the moment to the distribution function as follow

$$\rho = \int f d\mathbf{c} \qquad (7)$$

$$\rho \mathbf{u} = \int \mathbf{c} f d\mathbf{c} \qquad (8)$$

$$T = \int g d\mathbf{c}. \qquad (9)$$

By applying the Chapmann-Enskog expansion, Eqs. (1) to (9) can lead to the macroscopic continuity, momentum and energy equation. Detail derivation can be found in Azwadi *et al.* (Azwadi *et al.*, 2007).

$$\nabla \cdot \mathbf{u} = 0 \tag{10}$$

$$\frac{\partial \mathbf{u}}{\partial t} + \mathbf{u}\nabla \cdot \mathbf{u} = -\frac{1}{\rho}\nabla p + \upsilon\nabla^2 \mathbf{u} + F \tag{11}$$

$$\frac{\partial T}{\partial t} + \nabla \cdot (uT) = \chi\nabla^2 T \tag{12}$$

The viscosity ν and thermal diffusivity χ are related to the time relaxation as follow

$$\upsilon = \frac{\tau_f}{3} \tag{13}$$

$$\chi = \tau_g \tag{14}$$

CUBIC-INTERPOLATED-PSEUDO-PARTICLE (CIP)

The CIP method was proposed and has been highly proven to be a universal solver for hyperbolic type of equations (Takewaki *et al*.). CIP is known as a numerical method for solving advection equation with low numerical diffusion (Yuya *et al*., 2004). This method constructs a solution inside the grid cell close enough to the real solution of the given equation (Yabe *et al*., 2002).

In this section, we briefly discuss the theory of CIP scheme in one dimensional case. For higher dimensional cases, readers are encouraged to refer the cited references. We consider a linear hyperbolic equation to be solved in the following term

$$\frac{\partial f}{\partial t} + c\frac{\partial f}{\partial x} = 0 \tag{15}$$

The theoretical solution of Eq. (15) is obtained by shifting a profile

$$f(x_i, t + \Delta t) = f(x_i - c\Delta t, t) \tag{16}$$

$$F_i(x) = A_i(x - x_i)^3 + B_i(x - x_i)^2 + C_i(x - x_i) + D_i \qquad (17)$$

The coefficients of *A, B, C* and *D* are determined so that the interpolation function and its first derivatives is continuous at both ends. As a result, we have

$$A_i = \frac{g_i + g_{i-1}}{\Delta x^2} + \frac{2(f_i - f_{i-1})}{\Delta x^3} \qquad (18)$$

$$B_i = \frac{3(f_{i-1} - f_i)}{\Delta x^2} + \frac{2g_i + g_{i-1}}{\Delta x} \qquad (19)$$

$$\frac{F_i(x_i)}{dx} = C_i = g_i \qquad (20)$$

$$F_i(x_i) = D_i = f_i \qquad (21)$$

Once $F_i(x)$ are determined for all grid intervals, the spatial derivatives are calculated as

$$\frac{F_i(x_i)}{dx} = \left(3A_i(x - x_i) + 2B_i\right)(x - x_i) + g_i \qquad (22)$$

The advection profile is given by

$$f_i^{n+1} = A_i \xi^3 + B_i \xi^2 + g_i^n \xi + f_i^n \qquad (23)$$

and

$$g_i^{n+1} = 3A_i \xi^2 + 2B_i \xi + g_i^n \qquad (24)$$

where

$$f^{n+1} = F(x - c\Delta t) \qquad (25)$$

$$g^{n+1} = \frac{dF(x - c\Delta t)}{dx} \qquad (26)$$
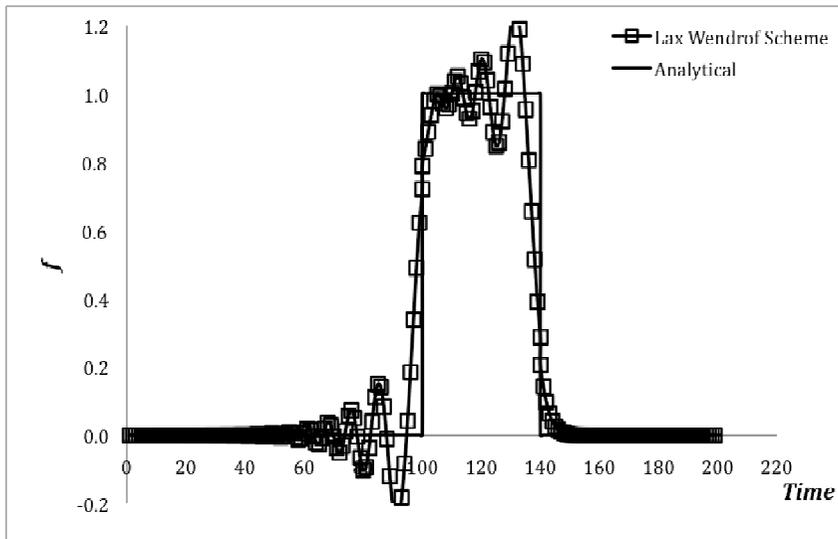
$$\xi = -c\Delta t \qquad (27)$$

We first apply CIP method to the propagation of a square wave. Figure 2 shows the comparison of results when the wave moves from its initial position to new position predicted by CIP, first order upwind scheme, Lax Wendroff Scheme and the analytical solution. The result shows that the CIP method gives the best solution compared to other methods.
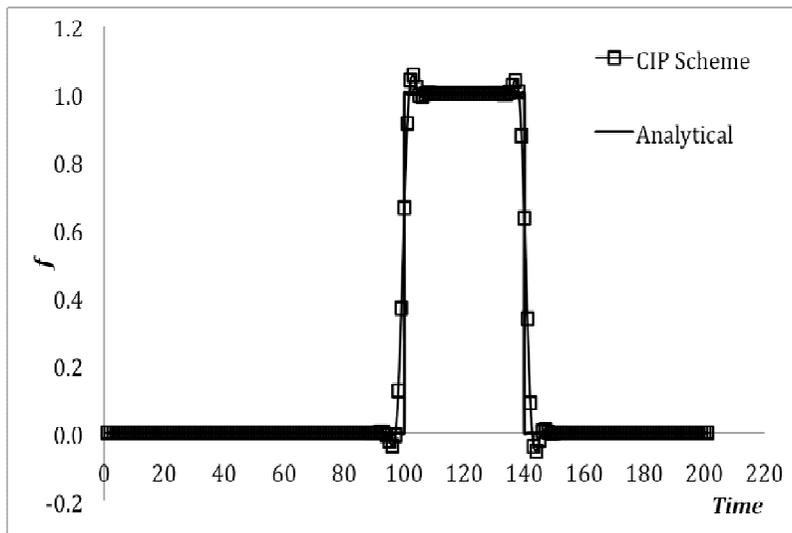
(a)
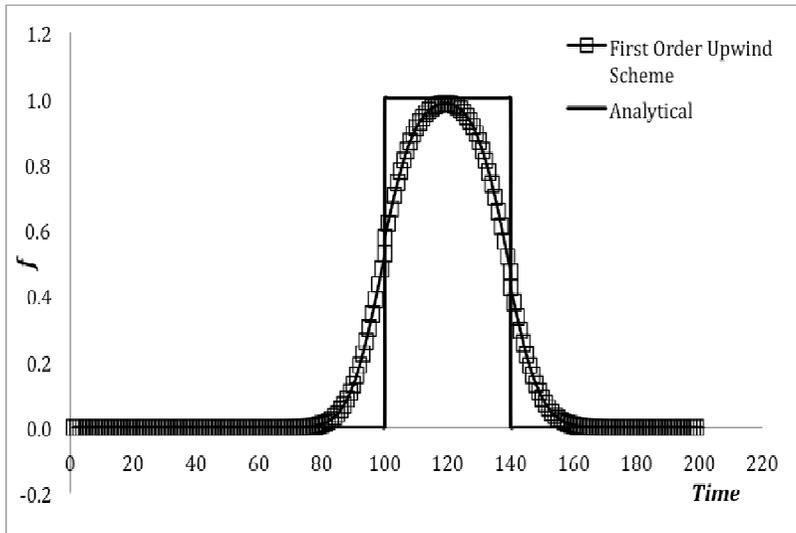
(b)

(c)

Figure 2: Comparison solution to the advection equation using (a) CIP scheme (b) first order upwind scheme and (c) Lax-Wendroff scheme

TWO-DIMENSIONAL CIP-LBM THERMAL BGK BOLTZMANN SCHEME

The LBM governing equation is readily split into advection and non-advection phase. The non-advection phase or collision term specifically, can be directly solved without any difficulty. On the other hand, the advection phases can be solved using CIP method discussed in the previous section.

Two dimensional Boltzmann equations is expressed as

$$\frac{\partial f}{\partial t} + c_x \frac{\partial f}{\partial x} + c_y \frac{\partial f}{\partial y} = -\frac{1}{\tau_f}\left(f - f^{eq}\right) + F \tag{28}$$

$$\frac{\partial g}{\partial t} + c_x \frac{\partial g}{\partial x} + c_y \frac{\partial g}{\partial y} = -\frac{1}{\tau_g}\left(g - g^{eq}\right) \tag{29}$$

The evolution of the advection and collision phase can be rewritten separately as follow

$$\frac{\partial f}{\partial t} + c_x \frac{\partial f}{\partial x} + c_y \frac{\partial f}{\partial y} = 0 \tag{30}$$

$$\frac{\partial g}{\partial t} + c_x \frac{\partial g}{\partial x} + c_y \frac{\partial g}{\partial y} = 0 \tag{31}$$

$$\frac{\partial f}{\partial t} = -\frac{1}{\tau_f}\left(f - f^{eq}\right) + F \tag{32}$$

$$\frac{\partial g}{\partial t} = -\frac{1}{\tau_g}\left(g - g^{eq}\right) \tag{33}$$

Differentiating Eqs. (30) to (33) respect to x and y gives

$$\frac{\partial}{\partial t} f_x + c_x \frac{\partial}{\partial x} f_x + c_y \frac{\partial}{\partial y} f_x = 0 \tag{34}$$

$$\frac{\partial}{\partial t} f_y + c_x \frac{\partial}{\partial x} f_y + c_y \frac{\partial}{\partial y} f_y = 0 \tag{35}$$

$$\frac{\partial}{\partial t} g_x + c_x \frac{\partial}{\partial x} g_x + c_y \frac{\partial}{\partial y} g_x = 0 \tag{36}$$

$$\frac{\partial}{\partial t} g_y + c_x \frac{\partial}{\partial x} g_y + c_y \frac{\partial}{\partial y} g_y = 0 \tag{37}$$

$$\frac{\partial}{\partial t} f_x = -\frac{1}{\tau_f} \left(f_x - f_x^{eq} \right) + F_x \tag{38}$$

$$\frac{\partial}{\partial t} f_y = -\frac{1}{\tau_f} \left(f_y - f_y^{eq} \right) + F_y \tag{39}$$

$$\frac{\partial}{\partial t} g_x = -\frac{1}{\tau_g} \left(g_x - g_x^{eq} \right) \tag{40}$$

$$\frac{\partial}{\partial t} g_y = -\frac{1}{\tau_g} \left(g_y - g_y^{eq} \right) \tag{41}$$

where

$$f_x = \frac{\partial f}{\partial x}, \ f_y = \frac{\partial f}{\partial y} \ , \ g_x = \frac{\partial g}{\partial x}, \text{ and } g_y = \frac{\partial g}{\partial y}.$$

In CIP method, the profile between lattice points for density distribution function is interpolated using cubic polynomial as follow

$$F_{i,j}(x,y) = \left[\left(A1_{i,j} X + A2_{i,j} Y + A3_{i,j} \right) X + A4_{i,j} Y + \partial_x f_{i,j} \right] X$$
$$+ \left[\left(A5_{i,j} Y + A6_{i,j} X + A7_{i,j} \right) Y + \partial_y f_{i,j} \right] Y + f_{i,j} \tag{42}$$

where $X = x - x_{i,j}$ and $Y = y - y_{i,j}$. The coefficients in Eq. (42) are expressed as follow

$$A1_{i,j} = \left[-2d_i + \partial_x \left(f_{i+1,j} + f_{i,j} \right) \Delta x \right] / \Delta x^3 \tag{43}$$

$$A2_{i,j} = \left[A8_{i,j} - \partial_x d_j + \partial_x \Delta x\right]\!\big/ \Delta x^2 \Delta y \tag{44}$$

$$A3_{i,j} = \left[3d_i - \partial_x \left(f_{i+1,j} + 2f_{i,j}\right)\!\Delta x\right]\!\big/ \Delta x^2 \tag{45}$$

$$A4_{i,j} = \left[-A8_{i,j} + \partial_x d_j \Delta x + \partial_y d_i \Delta y\right]\!\big/ \Delta x \Delta y \tag{46}$$

$$A5_{i,j} = \left[-2d_j + \partial_y \left(f_{i,j+1} + f_{i,j}\right)\!\Delta y\right]\!\big/ \Delta y^3 \tag{47}$$

$$A6_{i,j} = \left[A8_{i,j} - \partial_y d_i \Delta x\right]\!\big/ \Delta x \Delta y^2 \tag{48}$$

$$A7_{i,j} = \left[3d_j - \partial_y \left(f_{i,j+1} + 2f_{i,j}\right)\!\Delta y\right]\!\big/ \Delta y^2 \tag{49}$$

$$A8_{i,j} = f_{i,j} - f_{i+1,j} - f_{i,j+1} + f_{i+1,j+1} \tag{50}$$

where

$$d_i = f_{i+1,j} - f_{i,j} \text{ and } d_j = f_{i,j+1} - f_{i,j}$$

The spatial derivatives are then calculated as

$$F_{x(i,j)}(x,y) = \left(3A1_{i,j}X + 2A2_{i,j}Y + 2A3_{i,j}\right)X + \left(A4_{i,j} + A6_{i,j}Y\right) + f_{x,i,j} \tag{51}$$

$$F_{y(i,j)}(x,y) = \left(A2_{i,j}X + A4_{i,j}\right)X + \left(3A5_{i,j}Y + 2A6_{i,j}X + 2A7_{i,j}\right)Y + f_{y,i,j} \tag{52}$$

Finally, the advected profile for density distribution function is approximated as follows

$$f_{i,j}^{n*} = F_{i,j}\left(x_{i,j} + \xi_x, y_{i,j} + \xi_y\right) \tag{53}$$
$$f_{x(i,j)}^{n*} = F_{x(i,j)}\left(x_{i,j} + \xi_x, y_{i,j} + \xi_y\right) \tag{54}$$

$$f_{y(i,j)}^{n*} = F_{y(i,j)}\left(x_{i,j} + \xi_x, y_{i,j} + \xi_y\right) \tag{55}$$

where $\xi_x = -c_{x,i}\Delta t$ and $\xi_y = -c_{y,i}\Delta t$.

The same procedures apply for the internal energy distribution function.

The evolution of CIP-LBM consists of three steps. The initial value of f, f_x, f_y and g, g_x and g_y are specified at each grid point (i, j). Then the system evolves in the following steps;

1. Since the pre-advected value of f, f_x, f_y and g, g_x and g_y are known on each grid, the cubic interpolation process can be completed according to Eqs. (42), (51) and (52).

2. After the interpolation, advection takes place and f^{n+1}, f_x^{n+1}, f_y^{n+1}, g^{n+1}, g_x^{n+1}, and g_y^{n+1} on the grids are obtained using Eqs. (53) to (55).

3. The values of f^{n+1}, f_x^{n+1}, f_y^{n+1}, g^{n+1}, g_x^{n+1}, and g_y^{n+1} at the grid intervals are computed again from Eqs. (42), (51) and (52). These interpolation and advection processes are repeated one after another until the convergence criterion is satisfied.

RESULTS AND DISCUSSION

In present study, the proposed CIP-thermal LBM was used to simulate the natural convection heat transfer in a two dimensional square cavity with the left wall is kept at hot temperature and right wall at cold temperature. Top and bottom walls of the cavity are being adiabatic. Temperature gradient exists in a fluid due to temperature difference. Consequently, the density difference induces a fluid motion that is convection.

Schematic diagram of the setup simulation is shows in Figure 3. No-slip boundary conditions (Frish *et al*., 1986) are imposed on all the faces of the square with height, *H*. The thermal conditions applied on the walls are depicted in Figure 3.

$$\frac{\partial T}{\partial y} = 0$$

T_H **g** T_C
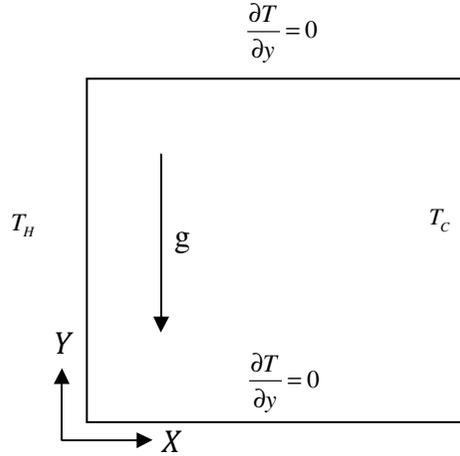
Y

$$\frac{\partial T}{\partial y} = 0$$

X

Figure 3: Geometry and boundary conditions of the natural convection heat transfer in a square cavity problem.

In the simulation, the Boussinesq approximation is applied to the buoyancy term. With this approximation, it is assumed that all fluid properties can be considered as constant in the body force term except for the temperature dependence of the density. The Boussinesq approximation equation can be written as

$$\rho G = \rho \beta g (T - T_m)\mathbf{j} \tag{56}$$

where β is the thermal expansion coefficient, g is the acceleration due to the gravity, T_m is the average temperature and j is the vertical direction opposite to that of gravity. Therefore, the external force in Eq. (1) can be written as

$$F = 3G(c_y - v)f_i^{eq} \tag{57}$$

The dynamical similarity depends on two dimensionless parameters; the Prandtl number, Pr and the Rayleigh number, Ra;

$$\Pr = \frac{\upsilon}{\chi}, Ra = \frac{g\beta\Delta T L^3}{\upsilon\chi} \tag{58}$$

The convergence criterion for all the tested cases is

$$f_i^{eq,n+1} - f_i^{eq,n} \leq 10^{-5} \tag{59}$$

$$g_i^{eq,n+1} - g_i^{eq,n} \leq 10^{-5} \tag{60}$$

In the simulation, Pr is set to be 0.71 to simulate air as a working fluid. In this study, the number of grid is taken uniform in both *x*-and *y*-direction. The grid dependence study has been done for the simulation at Ra = 10^3 and shown in Table 1. As we can see from the table, as we increase the grid size, the calculated variables converge to a fixed value. Grid size of 51 x 51 is found to be sufficient compare to Azwadi *et al.* (Azwadi *et al.*, 2007) where the grid size of 101 x 101 was needed to simulate the same phenomena at same Rayleigh number. For Ra = 10^4, grid size of 71 x 71 was used for the simulation while Azwadi *et al.* (Azwadi *et al.*, 2007) applied grid size of 151 x 151 for the same simulation. These comparisons indicate that the grid size can be reduced about 50 percent by using CIP-LBM scheme.

TABLE 1: Grid dependence study of Ra = 10^3.

Grid	31 x 31	51 x 51	61 x 61
U_{max}	3.598	3.632	3.649
Y	0.806	0.820	0.820
V_{max}	3.701	3.694	3.739
X	0.19	0.19	0.18
Nu_{ave}	1.112	1.116	1.117

The main characteristic of natural convection flow are shown in terms of streamlines and isotherms. Figure 4 illustrates the streamline patterns for all Rayleigh numbers simulated using CIP-LBM, excellent agreement were obtained with those from previous studies by Davis *et al.* (Davis *et al.,*1983).
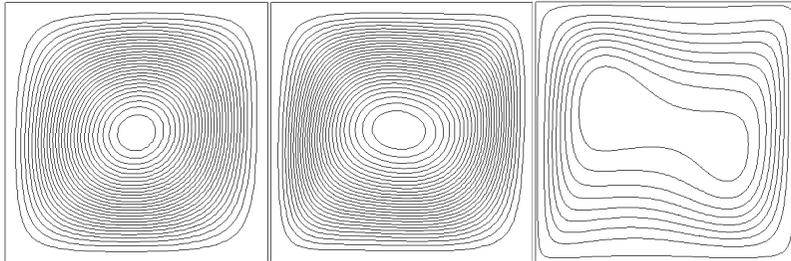
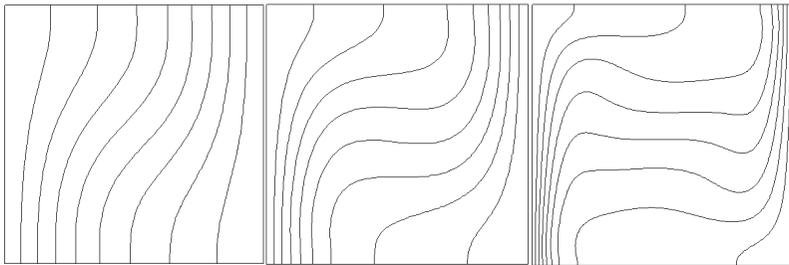Figure 4: Streamline plots for Ra = 10^3, 10^4 and 10^5

Figure 5: Isotherms for Ra = 10^3, 10^4 and 10^5

At Ra = 10^3, a circular shaped vortex appears at the centre of the cavity and the isotherms are almost vertically parallel to the wall indicating that conduction mode heat transfer mechanism is dominant.

By increasing the Rayleigh number to Ra = 10^4, circular vortex is distorted and evolved as a horizontally oval shaped vortex. Meanwhile, the isotherms start to be horizontally parallel to the wall at the center of cavity. This is due to the convection mode heat transfer and buoyancy effect. At this Rayleigh number, heat transfer mechanisms in the cavity are influenced by both convection and conduction mode.

For the simulation at high Rayleigh number (Ra = 10^5), two vortices exist when the system achieved steady state condition. Isotherms almost horizontally parallel to the wall indicating that convection is the main heat transfer mode.

Table 2 shows the numerical results of the maximum horizontal velocity on the vertical mid-plane of the cavity with its location, the

maximum vertical velocity on the horizontal mid-plane of the cavity with its location and also the average Nusselt number throughout the cavity using the CIP-LBM scheme. The numerical results obtained by the original internal energy thermal lattice Boltzmann model proposed by He *et al.* (He *et al.*,1998), simplified thermal model by Azwadi *et al.* (Azwadi *et al.*, 2007), Navier-Stokes solution by Davis *et al.* (Davis *et al.*, 1983) and the thermal LBM model proposed by Peng *et al.* (Peng *et al.*, 2003) are also included for comparison. As can be seen from the table, the prediction with CIPLBM method gives excellent agreement with others numerical method even at low spatial resolution.

TABLE 2: Comparison of the present CIP-LBM scheme numerical results with others numerical methods

Ra		10^3	10^4	10^5
U_{max}	He *et al.,* (1998)	3.649	16.156	34.245
	Azwadi *et al.,* (2007)	3.646	16.154	35.481
	Davis *et al.,* (1983)	3.634	16.182	34.810
	Peng *et al.,* (2003)	3.645	16.140	34.261
	Present	3.632	16.304	43.331
y	He *et al.,* (1998)	0.810	0.820	0.855
	Azwadi *et al.,* (2007)	0.810	0.820	0.855
	Davis *et al.,* (1983)	0.813	0.823	0.855
	Peng *et al.,* (2003)	0.810	0.820	0.855
	Present	0.820	0.82	0.9
V_{max}	He *et al.,* (1998)	3.700	19.679	68.276
	Azwadi *et al.,* (2007)	3.694	19.597	69.243
	Davis *et al.,* (1983)	3.679	19.509	68.220
	Peng *et al.,* (2003)	3.691	19.585	67.799
	Present	3.694	19.835	67.930
x	He *et al.,* (1998)	0.180	0.120	0.065
	Azwadi *et al.,* (2007)	0.180	0.120	0.065
	Davis *et al.,* (1983)	0.179	0.120	0.066
	Peng *et al.,* (2003)	0.180	0.120	0.065
	Present	0.190	0.13	0.066
Nu_{ave}	He *et al.,* (1998)	1.117	2.244	4.520
	Azwadi *et al.,* (2007)	1.117	2.236	4.549
	Davis *et al.,* (1983)	1.116	2.234	4.510
	Peng *et al.,* (2003)	1.117	2.235	4.511
	Present	1.116	2.201	4.249

The dimensionless horizontal and vertical velocity profile given at the mid-height and mid-width of the cavity are shown in Figure 6 and 7. Both figures show that the location of maximum velocity shifted nearer to

the walls if the Rayleigh number is increased. The magnitude of maximum velocity component is also directly proportional to the Rayleigh number.
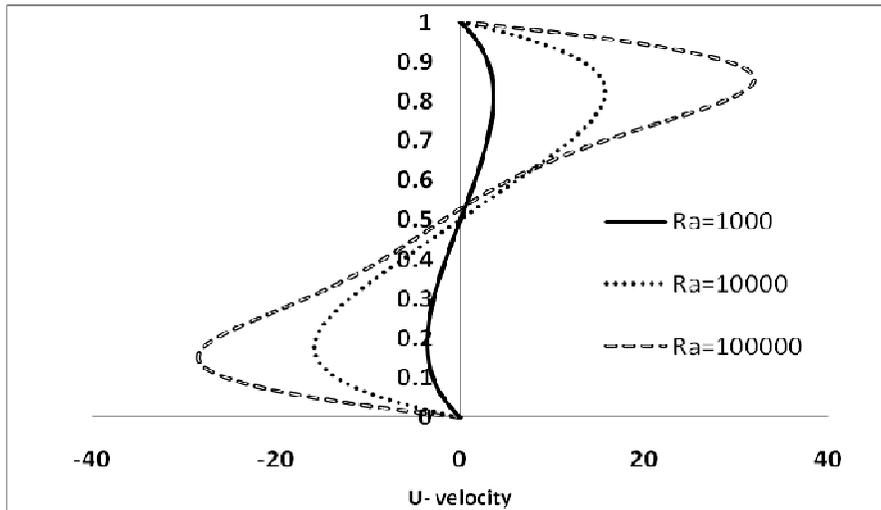

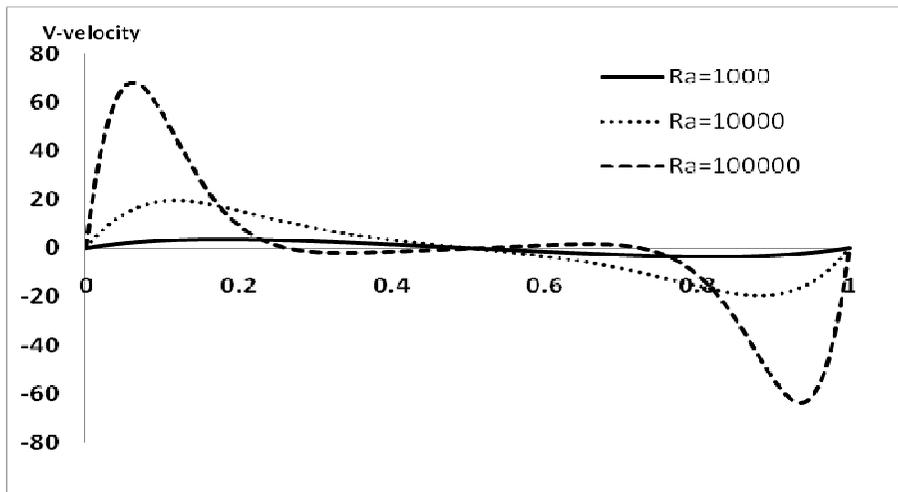Figure 6: Horizontal velocity profile at the mid height of the cavity

Figure 7: Vertical velocity profile at the mid width of the cavity.

CONCLUSION

In this paper, we solved the LB advection equation using CIP method. For the verification purpose, we simulated the natural convection heat transfer in a square cavity at various Rayleigh number. Our study showed that the flow pattern, heat transfer mechanism and Nusselt number are significantly affected by the value of Rayleigh number.

The demonstrated results are excellent agreement with those obtained from previous studies. This demonstrated that the proposed CIP-LBM is found to be an efficient and accurate numerical method for solving thermal fluid flow problem. The extension to 3D CIPLBM will be considered in our future study.

ACKNOWLEDGEMENTS

REFERENCES

Abe, T. 1998. Derivation of the Lattice Boltzmann Method by Means of the Discrete Ordinate Method for the Boltzmann Equation. *J. Comp. Phys.*, **131**: 241-246.

Azwadi C. S. N. 2007. The development of Simplified Thermal Lattice Boltzmann Models for the simulation of thermal fluid flow problems. *Phd. Thesis*. Keio University Japan.

Azwadi C.S. and Tanahashi, T. 2006. Simplified thermal lattice Boltzmann model in incompressible limit. *Proc. Asean Cong. Fluid Mech.*, **11**: 275-280.

Baba Yuya, Akamatsu Fumiteru and Katsuki Masashi. 2004. CIP characteristic in Direct Simulations. *JSME Intl. J Series B*, **47**(4): 750-760.

Bernsdorf, J., Brenner, G. and Durst, F. 2000. Numerical analysis of the pressure drop in porous media flow with Lattice Boltzmann (BGK) automata. *Comp. Phys. Comm.*, **129**: 247-255.

Bhatnagar, P. L., Gross, E. P. and Krook, M. 1954. A model for collision process in gasses 1. Small amplitude process in charged and neutral one component system. *Phys. Rev.* **94**: 511-525.

Cao, N., Chen, S., Jin, S. and Martinez, D. 1997. Physical symmetry and lattice symmetry in the Lattice Boltzmann method. *Phys. Rev. E*, **55**: 21-24.

Chen, S., Chen, H., Martinez, D. and Matthaeus, W.H. 1991. Lattice Boltzmann model for simulation of magnetohydrodynamics. *Phys. Rev. Lett.*, **67**: 3776-3779.

Davis, D. V. 1983. Natural Convection of air in a square cavity: A benchmark numerical solution. *Intl. J. Numer. Method Fluid*, **3**: 249-264.

Frish, U., Hasslacher, B. and Pomeau, Y. 1986. Lattice-Gas Automata for the Navier-Stokes Equation. *Phys. Rev. Lett.*, **56**: 1505-150.

He, Xiaoyi, Chen, Shiyi, and Doolen, Gary D. 1998. A Novel Thermal Model for the Lattice Boltzmann Method in Incompressible Limit. *J. Comp. Phys.* **146**: 282–300.

Luo, L. S. and He, X. 1997. Velocity and density profiles of granular flow in channels using a lattice gas automaton. *Phys. Rev. E*, **55**: 6811-6817.

Martys, N. S. and Chen, H. 1996. Simulation of multicomponent fluid in complex three dimensional geometries by the lattice Boltzmann method. *Phys. Rev. E*, **53**: 743-750.

Nor Azwadi C. S. and Tanahashi, T. 2008. Simplified Finite Difference Thermal Lattice Boltzmann Method. *Int. J. of Modern Phys.B*, **22**(22): 3865-3876.

Peng, Y., Shu, C. and Chew, Y.T. 2003. Simplified thermal lattice Boltzmann for incompressible thermal flow. *Phys. Rev. E*, **68**: 026701-026708.

Reider, M. B. and Sterling, J. D. 1995. Accuracy of discrete velocity BGK models for the simulation of the incompressible Navier Stokes equation. *Computational and Fluids*, **24**: 459-467.

Takewaki, H., Nishigushi, A. and Yabe, T. Cubic Interpolated Pseudo-Particle Method (CIP) for Solving Hyperbolic Type equation. National Institute for Fusion Science. NII- Electronic Library Services.

Tolke, J., Krafczvk, M., Schulz, M., Rank, E. and Berrios, R. 1998. Implicit discretization and nonuniform mesh refinement approaches for FD discretizations of LBGK Models. *Intl J. Mod. Phys. C*, **9**: 1143-1157

Yabe, T., Ogata, Y., Takizawa, K., Kawai, T., Segawa, A. and Sakurai, K. 2002. The next generation CIP as a conservative semi-Lagrangian solver for solid, liquid and gas. *J. of Comp. and App. Math.*, **149**(1): 267-277

Yabe, T., Xiao Feng and Utsumi Takayuki. 2001. The constrained interpolation profile method for multiphase analysis. *J. Comp. Phys*. **169**: 556–593.